Electronic Supplementary Material (ESI) for Journal of Materials Chemistry A.

Supporting Information

Copper nanoparticles embedded in triphenylamine functionalized bithiazole-metal complex as active photocatalysts for visible light-driven hydrogen evolution

Jingpei Huo and Heping Zeng*

State Key Laboratory of Luminescent Materials and Devices, Institute of Functional Molecules, School of Chemistry and Chemical Engineering, South China University of Technology, Guangzhou, 510641, P. R. China

*Corresponding Author E-mail: hpzeng@scut.edu.cn; fax: 8620-87112631.

Experimental section

Materials

All the reagents and solvents were analytical grade and used as received.[1] Among them, Tetrabutylammonium hexafluorophosphate ($TBAPF_6$, ≥ 99.0%) was purchased from J&K Chemical Ltd. Copper (II) acetylacetonate (≥ 99.9%) and oleylamine (70%) was purchased from Sigma-Aldrich Co. LLC.[2] Starting from hydroxyacetophenone (99%), iodomethane (CH_3I, AR), rubeanic acid (99.0%), and 4-(Diphenylamino)phenylboronic acid (TPA, 98%) and copper(II) chloride ($CuCl_2$, 98%) as materials step by step, the complex Cu-2TPABTz (**Scheme S1**) was prepared according to the literature.[3] Besides, Nafion (5%) was purchased from J&K Chemical Ltd. E-pure deionized (DI) water (resistivity > 18 MΩ*cm) was achieved from a Millipore Milli-Q system.

Instruments

UV-visible (UV-vis) spectroscopy was carried out on a Hitachi U-3010 absorption spectrophotometer. Photoluminescence (PL) spectra was measured at room temperature on a Hitachi F-4500 fluorescence spectrophotometer with an excitation wavelength of 410 ± 5 nm. And the solid fluorescence quantum yields (ϕ_{PL}) values were measured by a calibrated integrating sphere system (λ_{ex} = 415 nm).[4]

The products were characterized by X-ray diffraction pattern (XRD) and recorded on a Bruker D8 Advance X-ray diffractometer (Bruker, Germany) with mono-chromatized Cu K_α radiation (λ = 0.15406 nm).

The morphology and structure were examined by transmission electron microscope (TEM, TecnaiG220, FEI) with an accelerating voltage of 200 kV, selected area electron diffraction (SAED),

and high-resolution transmission electron microscope (HR-TEM). Energy-dispersive X-ray (EDX) spectroscopy was obtained with an EDAX detector performed on the same HR-TEM.

X-ray photoelectron spectroscopy (XPS, Axis Ultra DLD, Kratos) analyses were performed by monochromatic X-ray source (Al K_{α}, 15 kV, 200 W).

The actual chemical compositions of the samples after the thorough purification were measured by means of inductively coupled plasma atomic emission spectrometry (ICP-AES, Prodigy, Leeman, LABS, Inc.).

Raman spectra were recorded on a micro-Raman spectrometer (Renishaw InVia) using a 514.5 nm excitation wavelength (Ar ion laser).

The Brunauer-Emmett-Teller (BET) specific surface area of photocatalysts was determined at liquid nitrogen temperature (77 K) with a Quantochrome NOVA 1200e instrument.

Time-resolved decay measurements were carried out at room temperature by using Edinburgh FLS 920 Fluorescence spectrometer.

The electron spin resonance (ESR) measurements were carried out with a ESR spectrometer (Bruker EMX-10). Prior to the measurements, the as-prepared samples separately immersed in an aqueous solution (2 mL) containing lactic acid (10%, v/v) was added to an in the cell, evacuated at 77 K to remove dissolved oxygen, and then irradiated for 30 min under visible light ($\lambda > 420$ nm) at room temperature. Meanwhile, ESR spectra obtained from the composite **3** without visible-light irradiation (Control) was shown in **Figure S8g**.

Photoelectrochemical and electrochemical impedance spectra (EIS) measurements were performed by electrochemical analyzer (CHI660C Instruments, Shanghai, China) with a standard three-electrode system. The film electrodes of Cu NPs loaded Cu-2TPABTz for the photoelectrochemical response and EIS measurements were prepared at first. The as-prepared sample was employed as working electrode, a Pt plate was used as a counter electrode and Ag/AgCl (saturates KCl) as a reference electrode separately. Lactic acid (10%, v/v) was mixed with Na_2SO_4 (0.5 mol*L^{-1}) aqueous solution as the

supporting electrolyte. Indiumtinoxide (ITO, 2*1 cm^2) with a thickness of 188 nm on a glass substrate was successively cleaned by acetone, methanol, isopropanol, and DI water in a sonicator, each for half an hour. The working electrodes were fabricated as follows: 0.05 g of the as-synthesized photocatalysts **1-5** and Cu-2TPABTz was respectively ground with 20 μL of a Nafion (5%) aqueous solution and 100 μL of ethanol to obtain slurry. The slurry was then spread onto ITO glass electrodes with an active area of 1.0 cm^2, and these electrolytes were dried at 120ºC for 1 h under nitrogen atmosphere to improve adhesion. All the resulting electrodes have the same film thickness of 15 μm. The scan rate of the current-voltage (*I-V*) and photocurrent-time response (*I-t*) spectrum is 10 $mV*s^{-1}$. The photocurrent densities produced at a bias of -0.1 V versus saturated calomel electrode (SCE) in the dark and light irradiation of 420 nm (light on/off cycles: 10s). The stability test was evaluated under the same condition (light on). The impedance spectroscopy of the materials was carried out under the open circuit voltage (VOC), and recorded over the frequency range of 0.1-10^5 Hz with an ac amplitude of 10 mV. Hereafter, based on the following Nernst equation, the potential of the photoelectrode versus the Ag/AgCl is converted to the reversible hydrogen electrode (RHE) potential.[5, 6]

$$E_{\mathrm{RHE}} = E_{\mathrm{Ag/AgCl}} + 0.059\mathrm{pH} + E^{\theta}_{\mathrm{Ag/AgCl}}$$

Where E_{RHE} is the converted potential *vs*. RHE, $E^{\theta}_{\mathrm{Ag/AgCl}} = 0.1976$ V at 25ºC, and $E_{\mathrm{Ag/AgCl}}$ is the experimental potential measured against the Ag/AgCl reference electrode.

Cyclic voltammetry (CV) was measured by a pyrex electrochemical cell consisting of a conventional three-electrode setup as mentioned above. $TBAPF_6$ and ferrocenium-ferrocene (Fc^+/Fc) were used as the supporting electrolyte and internal standard, respectively. All the potentials were measured at a scan rate of 100 $mV*s^{-1}$ for oxidation in N_2-purged dichloromethane and 100 $mV*s^{-1}$ for reduction in acetonitrile.

Typical procedure for the synthesis of composites 1-5[2, 7]

The preparation of Cu nanoparticles (NPs) was modified as followed. In a typical experiment, copper acetylacetonate (0.2618 g, 1 mmol) was dissolved in of oleylamine (20 mL) in a flask (50 mL). The solution was degassed for 1 h, and then protected under a flow of argon gas. The reactant mixture was heated to 250°C at a rate of 5°C/min with a magnetic stirrer. After reaction for 3 h, the product was cooled down to room temperature. The subsequent washing and surface modification processes were carried out in an argon-filled glovebox. All the solvents were degassed by using argon for 30 min. The product was washed with toluene and ethanol (v/v = 1:5) for three times and centrifuged at 10000 rpm for 20 min.

Aferwards, an appropriate amount of Cu NPs was added to 20 mL toluene and sonicated for 30 min to make Cu NPs disperse entirely. The as-synthesized **Cu-2TPABTz** was added to the above solution and continuous stirring for 3 h at room temperature, respectively. After volatilization of the toluene, the resulting powder was washed with ethanol and DI water for three times, and dried under vacuum at 60 °C for 12 h to acquire the Cu NPs hybridized complex samples. In addition, the composites **1-5** with different mass ratios of Cu NPs (from 1 to 15 wt%) were prepared by following the identical procedure as mentioned above.

Photocatalytic hydrogen production[8-10]

The photocatalytic reactions were performed by adopting a high-pressure Xe lamp (300 W) as an outer light source with a UV-cutoff filter and a Pyrex glass reaction cell, which was connected to a closed gas circulation and evacuated prior to each experiment. Briefly, the target photocatalyst (0.05 g) was suspended in a mixture of lactic acid (10 mL) and water (90 mL) for H_2 production. The

temperature of the reactant solution was kept constant with a water bath. The reaction-evolved H_2 were analyzed by a gas chromatograph (GC7900, Tian Mei, Shanghai) equipped with thermal conductivity detector (TCD) and high purity (99.999%) N_2 carrier gas.

Determination of QE values[11, 12]

Apparent quantum efficiency (QE) was measured under the same condition except for the incident mono-chromatic lights with different band-pass filters (λ = 420, 450, 480, 510, 540, 570, 600, 630 and 660 nm) and an irradiatometer. The incident photon number was obtained on a calibrated Si photodiode (SRC-1000-TC-QZ-N, Oriel), and the QE value was estimated by the following equation.

$$QE\% = \frac{2 \times \text{Number of evolved } H_2 \text{ molecules}}{\text{Number of incident photons}} \times 100\%$$

Table S1. Surface element composition of composite **3** before (a) and after (b) the recycling photocatalytic reactions determined by XPS

Sample	Element concentration (atom%)				
	C 1s	O 1s	Cu 2p	N 1s	S 2p
a	66.83	3.72	17.91	5.25	6.29
b	69.25	4.87	16.28	4.14	5.46

Table S2. Estimated band gap (E_g), energy levels of calculated conduction band (CB) and valence band (VB) edge at the point of zero charge for Cu-2TPABTz and composite **3**

Sample	Estimated energy band E_g (eV)	Calculated CB (eV)	Calculated VB (eV)
Cu-2TPABTz	2.67	-0.41	2.26
3	2.46	-0.62	1.84

References

1 I. Bonadies, F. Cimino, C. Carfagna and A. Pezzella, *Biomacromolecules*, 2015, **16**, 1667.

2 M. Shi, H. S. Kwon, Z. M. Peng, A. Elder and H. Yang, *ACS Nano*, 2012, **6**, 2157.

3 J. P. Huo and H. P.Zeng, *J. Mater. Chem. A*, 2015, **3**, 6258.

4 Z. L. Zhang, R. M. Edkins, J. Nitsch, K. Fucke, A. Steffen, L. E. Longobardi, D. W. Stephan, C. Lambert and T. B. Marder, *Chem. Sci*., 2015, **6**, 308.

5 Y.-S. Chen, J. S. Manser and P. V. Kamat, *J. Am. Chem. Soc*., 2015, **137**, 974.

6 L. Gao, Y. C. Cui, J. Wang, A. Cavalli, A. Standing, T. T. T. Vu, M. A. Verheijen, J. E. M. Haverkort, E. P. A. M. Bakkers and P. H. L. Notten, *Nano Lett*., 2014, **14**, 3715.

7 I. Shown, H.-C. Hsu, Y.-C. Chang, C.-H. Lin, P. K. Roy, A. Ganguly, C.-H. Wang, J.-K. Chang, C.-I. Wu, L.-C. Chen and K.-H. Chen, *Nano Lett*., 2014, **14**, 6097.

8 J. Liu, Y. Liu, N. Y. Liu, Y. Z. Han, X. Zhang, H. Huang, Y. Lifshitz, S.-T. Lee, J. Zhong and Z. K. Kang, *Science*, 2015, **347**, 970.

9 J. Z. Chen, X.-J. Wu, L. S. Yin, B. Li, X. Hong, Z. X. Fan, B. Chen, C. Xue and H. Zhang, *Angew. Chem. Int. Ed*., 2015, **54**, 1210.

10 J. P. Huo, L. T. Fang, Y. L. Lei, G. C. Zeng and H. P. Zeng, *J. Mater. Chem. A*, 2014, **2**, 11040.

11 X. H. Zhang, T. Y. Peng, L. J. Yu, R. J. Li, Q. Q. Li and Z. Li, *ACS Catal*., 2015, **5**, 504.

12 M. R. Gholipour, C.-T. Dinh, F. Béland and T.-O. Do, *Nanoscale*, 2015, **7**, 8187.

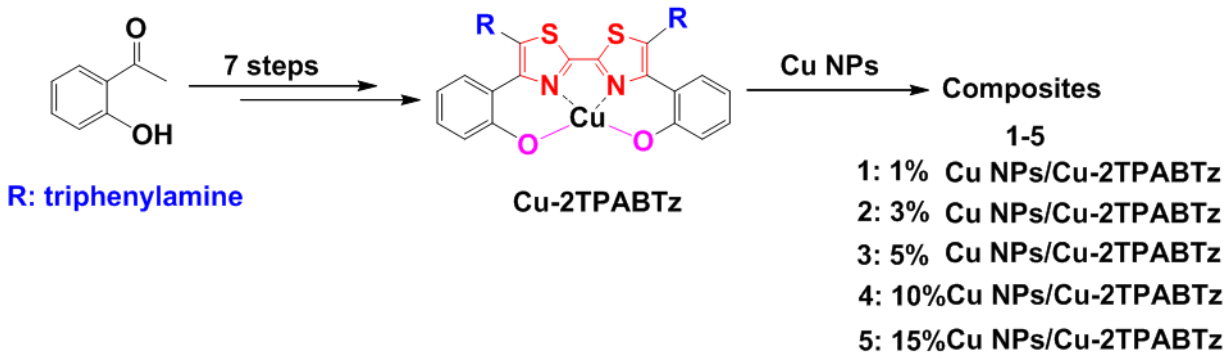

Scheme S1. Synthesis of triphenylamine functionalized bithiazole (**2TPABTz**)-based Cu complex and the corresponding composites **1-5**

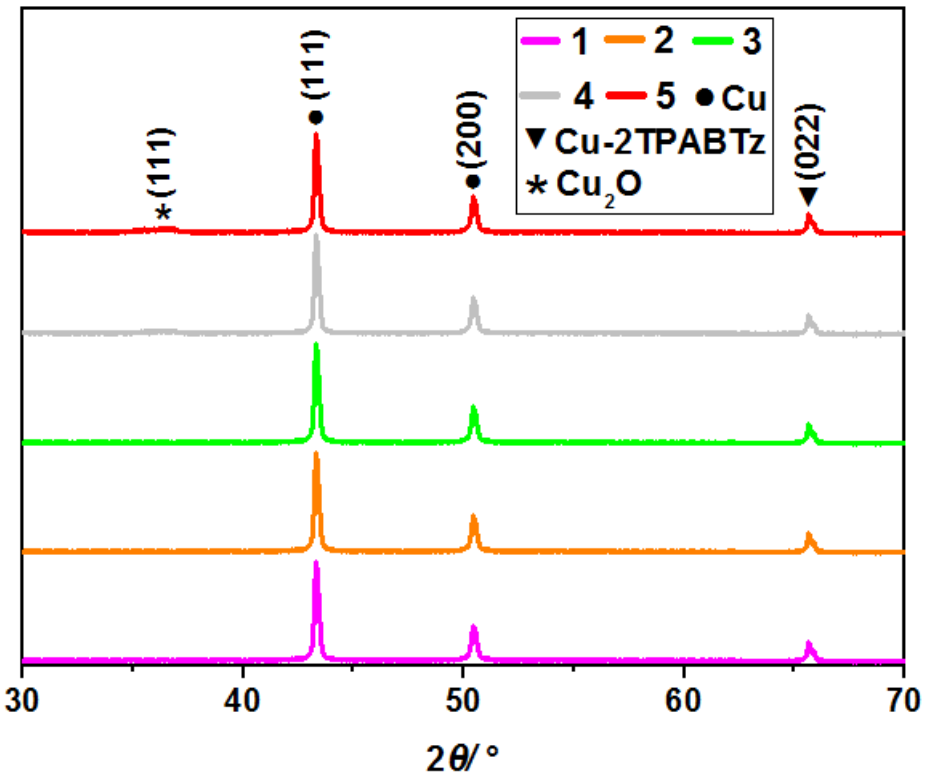

Figure S1. XRD patterns of the as-synthesized composites **1-5** with various Cu NPs concentrations.

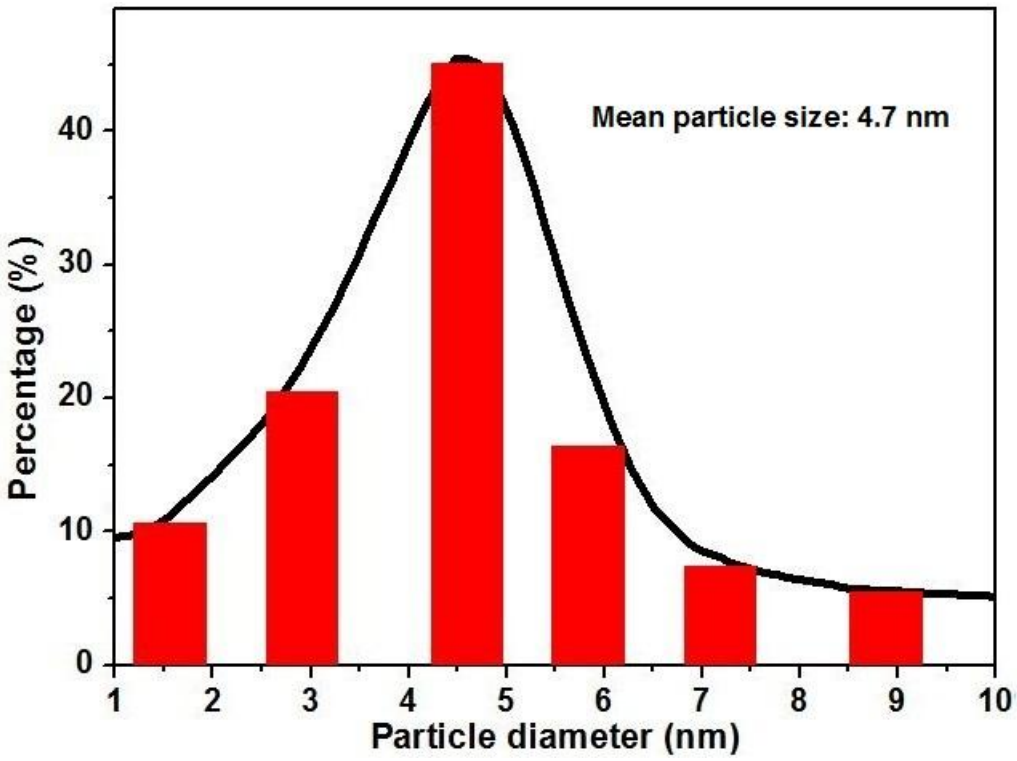

Figure S2. Cu NPs particle-size distribution of composite **3** (Mean particle size: 4.7 nm).

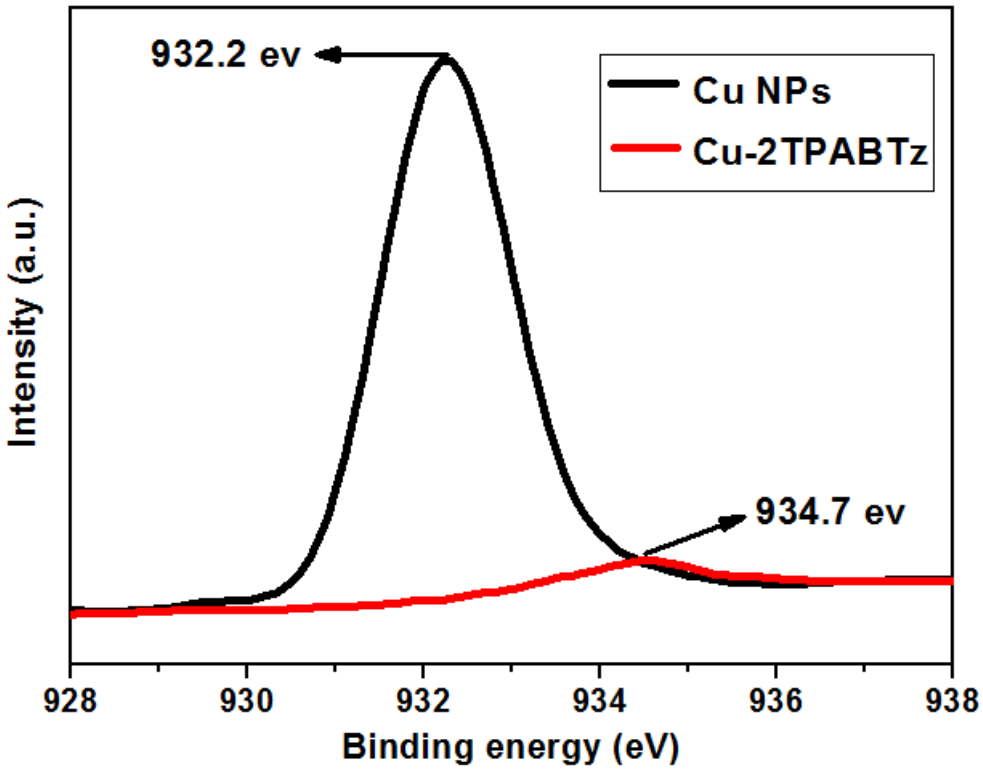

Figure S3. High-resolution XPS spectrum of the composite **3**.

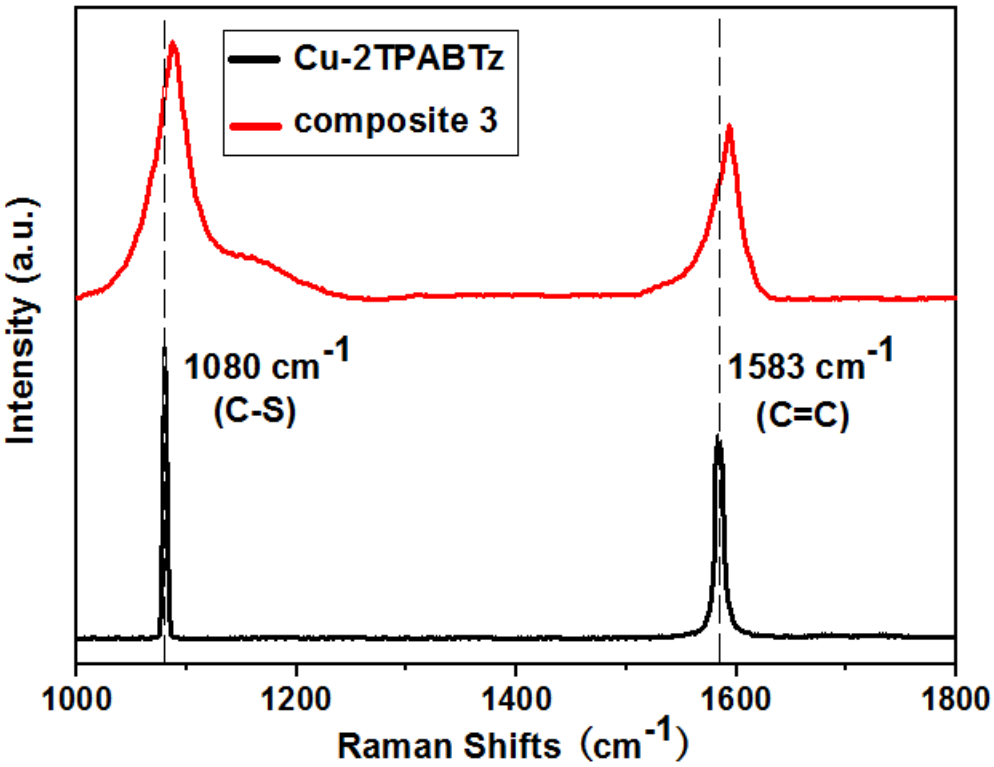

Figure S4. Raman spectra of the composite **3** and Cu-2TPABTz

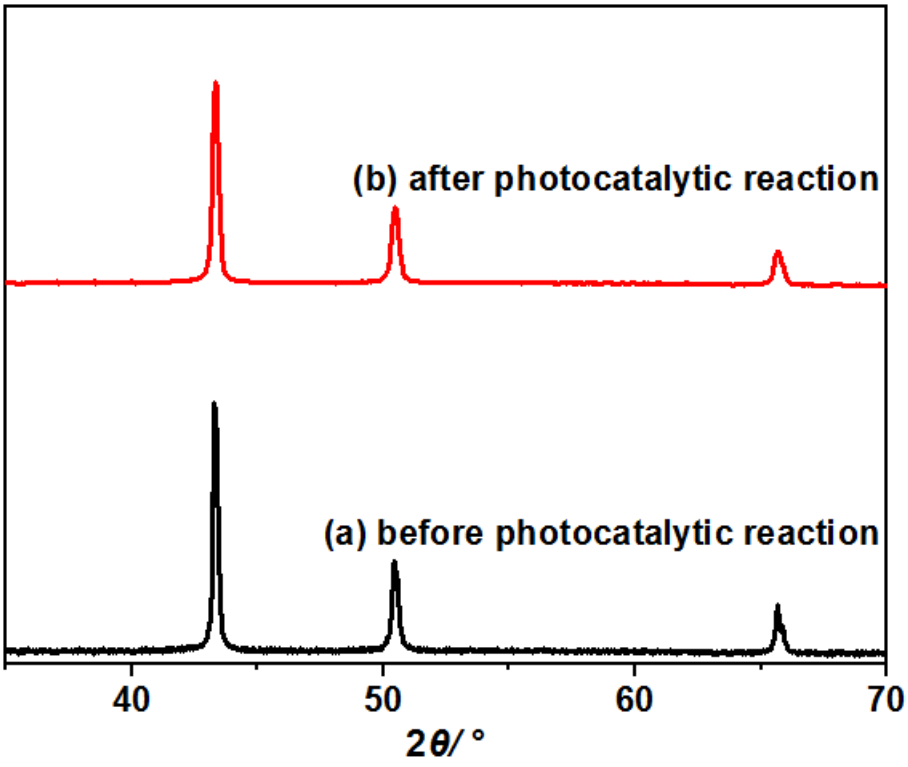

Figure S5. XRD patterns of composite **3** (5.0 wt% Cu NPs) before (a) and after (b) the recycling photocatalytic experiments.

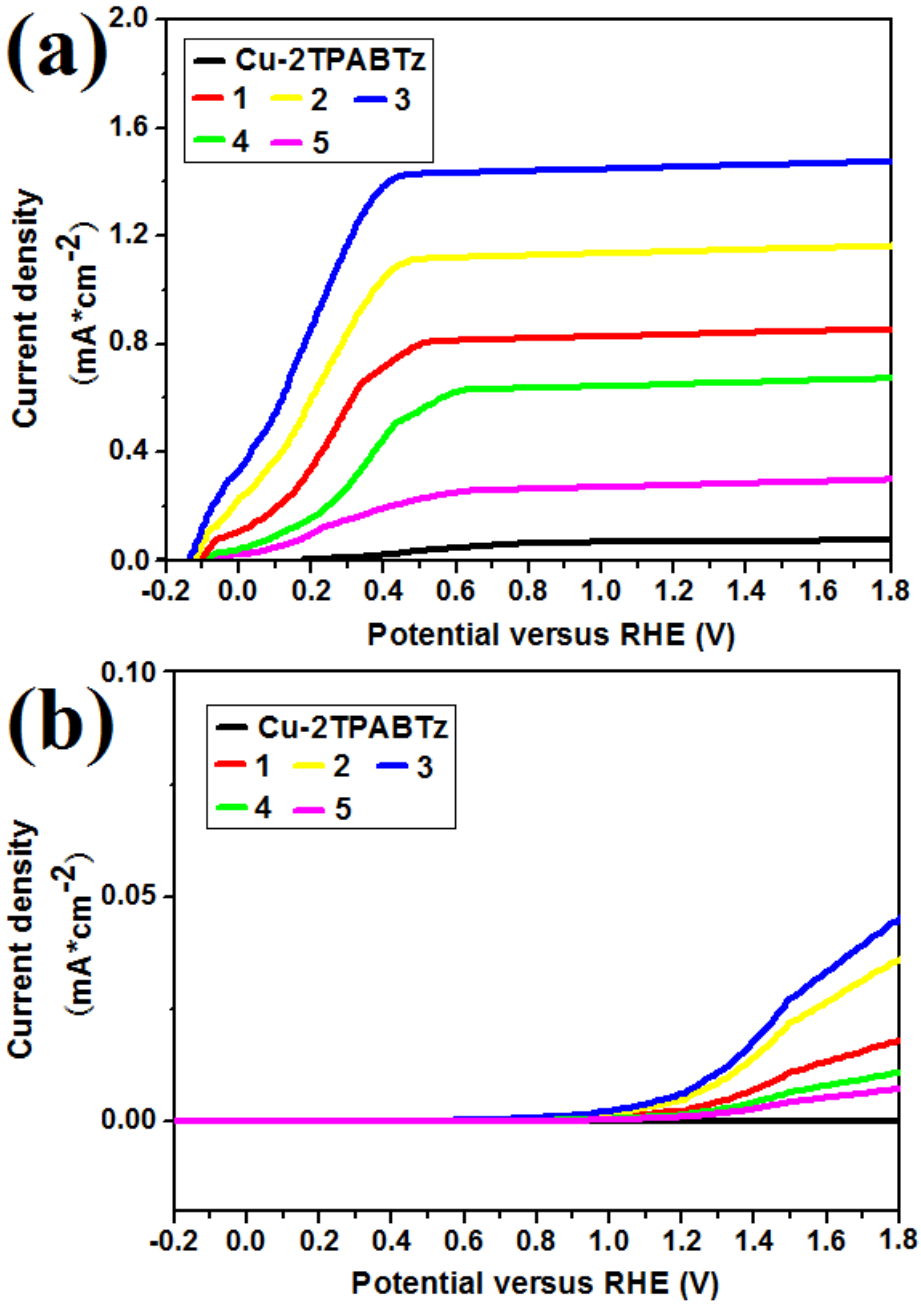

Figure S6. *I-V* curves of Cu-2TPABTz and the as-synthesized composites **1-5** under visible light irradiation (a) and in the dark condition (b).

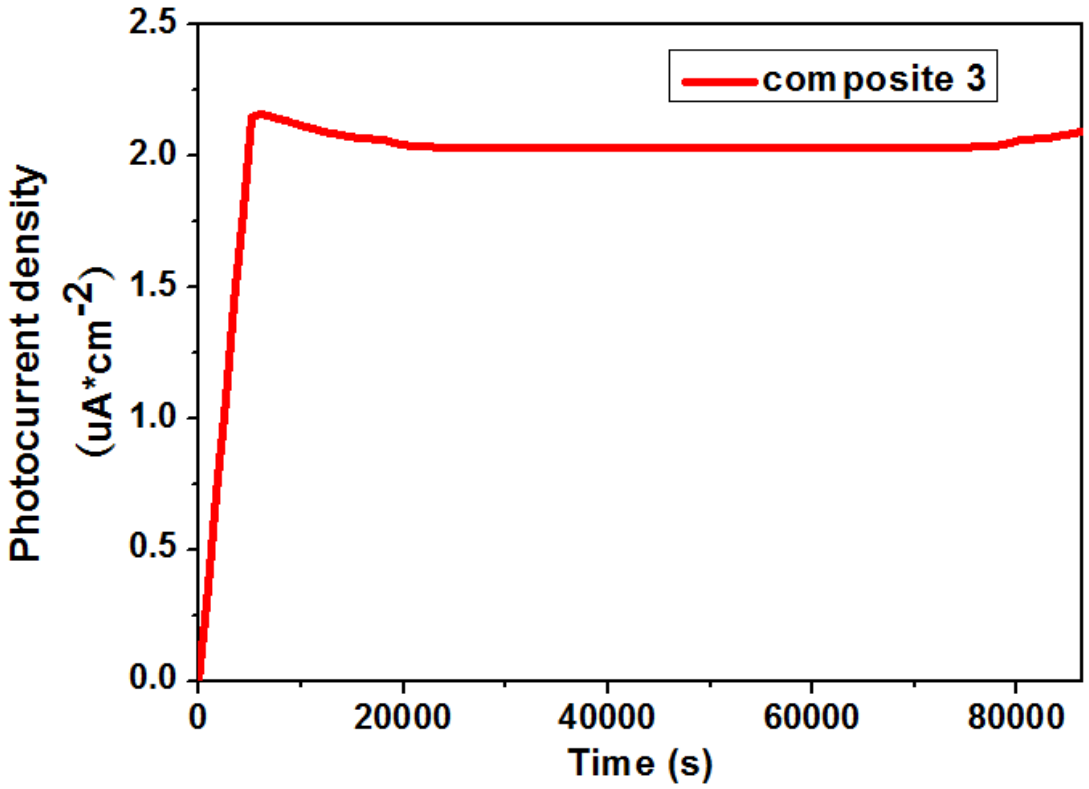

Figure S7. Prolonged photocurrent measurement of composite **3**.

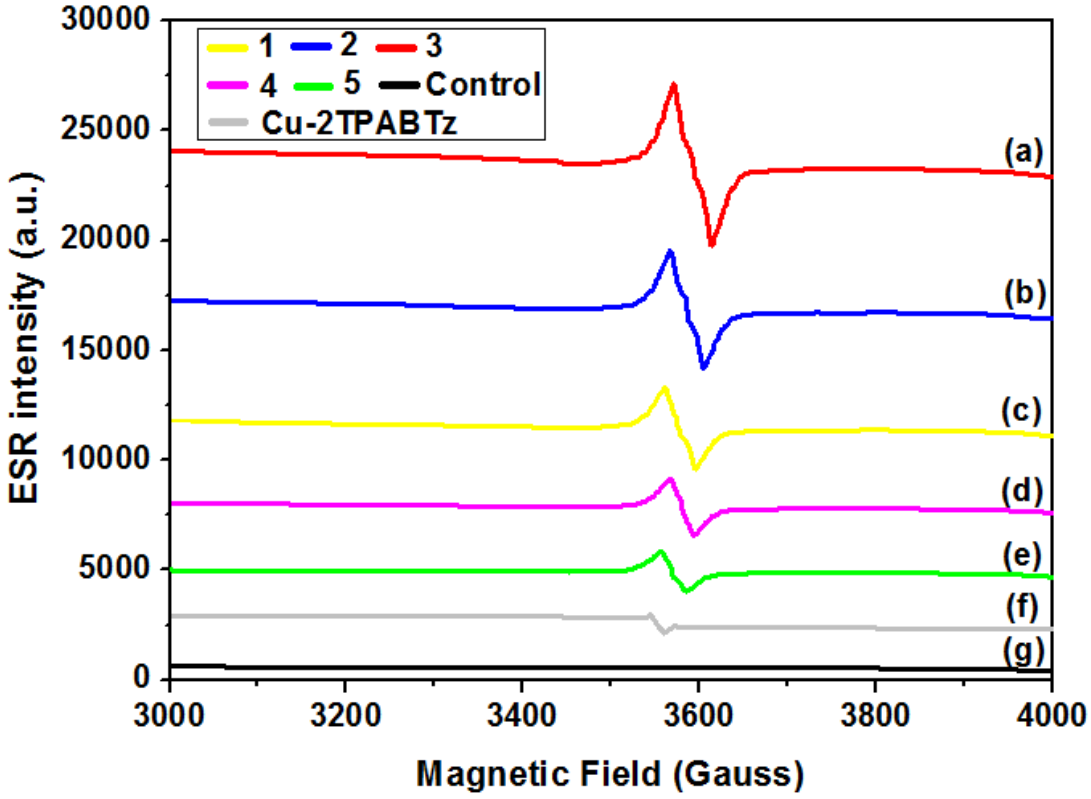

Figure S8. Experimental ESR spectrum of Cu-2TPABTz and the as-prepared composites **1**-**5**.

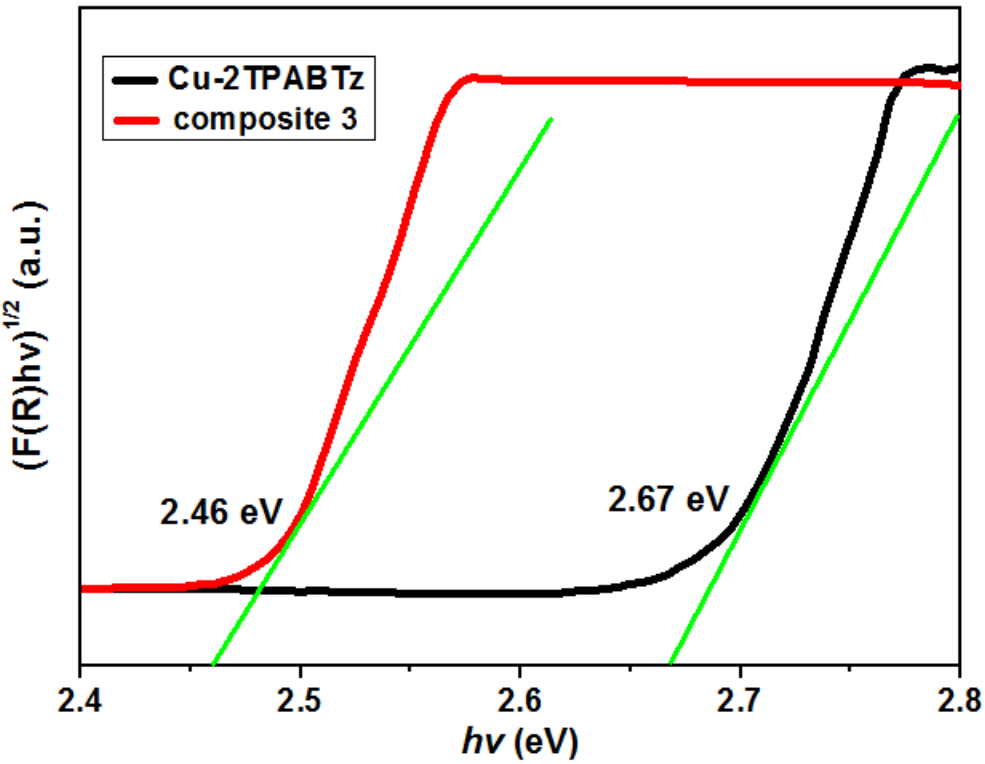

Figure S9. Tauc plots for Cu-2TPABTz and the as-prepared composite **3** under the direct transition assumption.